

Supporting Information

Rec. Nat. Prod. 17:2 (2023) 232-240

A New Monoterpene Alkaloid From the Stems of *Rauvolfia vomitoria*

Kailing Yang , Tao Yang , Xiaolei Li , Ruixi Zhou,

Rongkun Miao, Yuyan Guan, Yang Teng,

Guanqun Zhan and Zengjun Guo

¹ School of Pharmacy, Health Science Center, Xi'an Jiaotong University, Xi'an 710061, P. R. China

² School of Pharmacy, Jiamusi University, Jiamusi 154007, P. R. China

Table of Contents	Page
Figure S1: HR-ESI-MS spectrum of 1	3
Figure S2: ¹ H-NMR (600 MHz, CD ₃ OD) and ¹³ C-NMR (150 MHz, CD ₃ OD) spectrum of 1	4
Figure S3: HSQC spectrum of 1	5
Figure S4: HMBC spectrum of 1	5
Figure S5: HMBC spectrum of 1 (From δ_c 115 ppm to δ_c 160 ppm)	6
Figure S6: HMBC spectrum of 1 (From δ_c 25 ppm to δ_c 90 ppm)	6
Figure S7: ¹ H- ¹ H COSY spectrum of 1	7
Figure S8: ¹ H- ¹ H COSY spectrum of 1 (From δ_H 1.5 ppm to δ_H 4.0 ppm)	7
Figure S9: NOESY spectrum of 1	8
Figure S10: FT-IR spectrum of 1	8
Figure S11: UV Spectrum of 1	9
Figure S12: Scifinder search of new compound 1	9
Figure S13: ¹ H-NMR (600 MHz, CD ₃ OD) and ¹³ C-NMR (150 MHz, CD ₃ OD) spectrum of 2	10
Figure S14: ¹ H-NMR (600 MHz, CD ₃ OD) and ¹³ C-NMR (150 MHz, CD ₃ OD) spectrum of 3	11
Figure S15: ¹ H-NMR (600 MHz, CD ₃ OD) and ¹³ C-NMR (150 MHz, CD ₃ OD) spectrum of 4	12
Figure S16: ¹ H-NMR (600 MHz, CD ₃ OD) and ¹³ C-NMR (150 MHz, CD ₃ OD) Spectrum of 5	13
Figure S17: ¹ H-NMR (600 MHz, CD ₃ OD) and ¹³ C-NMR (150 MHz, CD ₃ OD) spectrum of 6	14
Figure S18: ¹ H-NMR (600 MHz, CD ₃ OD) and ¹³ C-NMR (150 MHz, CD ₃ OD) spectrum of 7	15
Figure S19: ¹ H-NMR (600 MHz, CD ₃ OD) and ¹³ C-NMR (150 MHz, CD ₃ OD) spectrum of 8	16
Figure S20: ¹ H-NMR (600 MHz, CD ₃ OD) and ¹³ C-NMR (150 MHz, CD ₃ OD) spectrum of 9	17
Figure S21: The inhibition rate curves of acetylcholinesterase inhibition activity	18

© 2022 ACG Publications. All rights reserved.

Figure S22: The inhibition rate curves of α -glucosidase inhibitory activity	18
Figure S23: The inhibition rate curves of DPPH radical scavenging activity	19
Figure S24: The inhibition rate curves of hydroxyl radical scavenging activity	19
Figure S25: The inhibition rate curves of FRAP activity	20
Table S1: The inhibitory rates of compounds 1–9 at the test concentrations	21
Table S2: Optical rotation values of 4–6	21

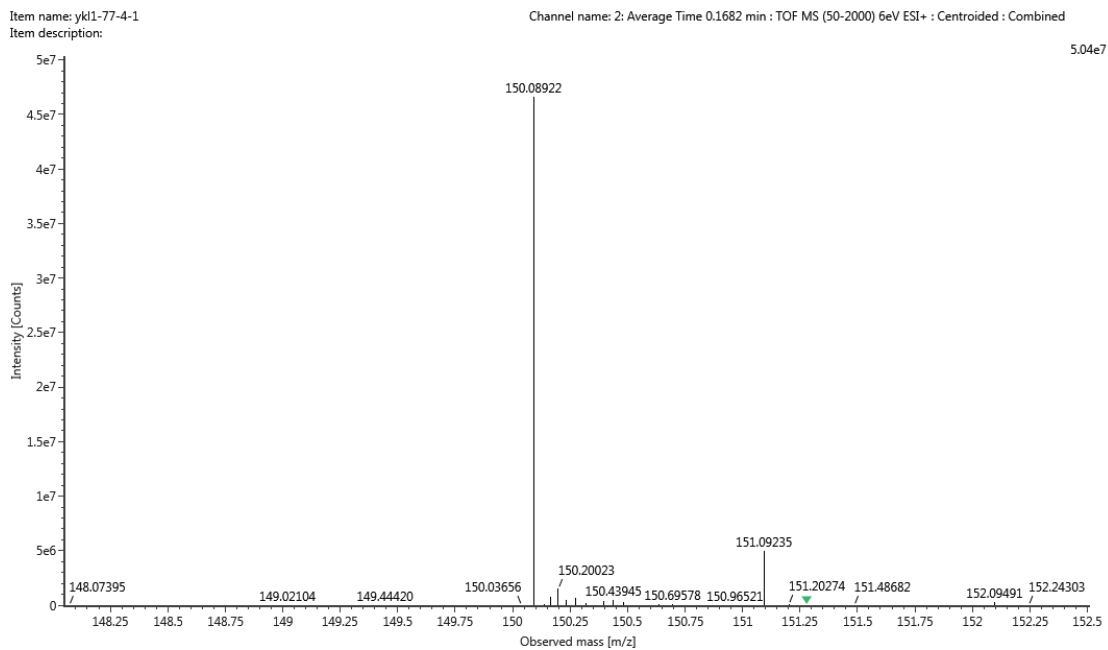


Figure S1: HR-ESI-MS spectrum of 1

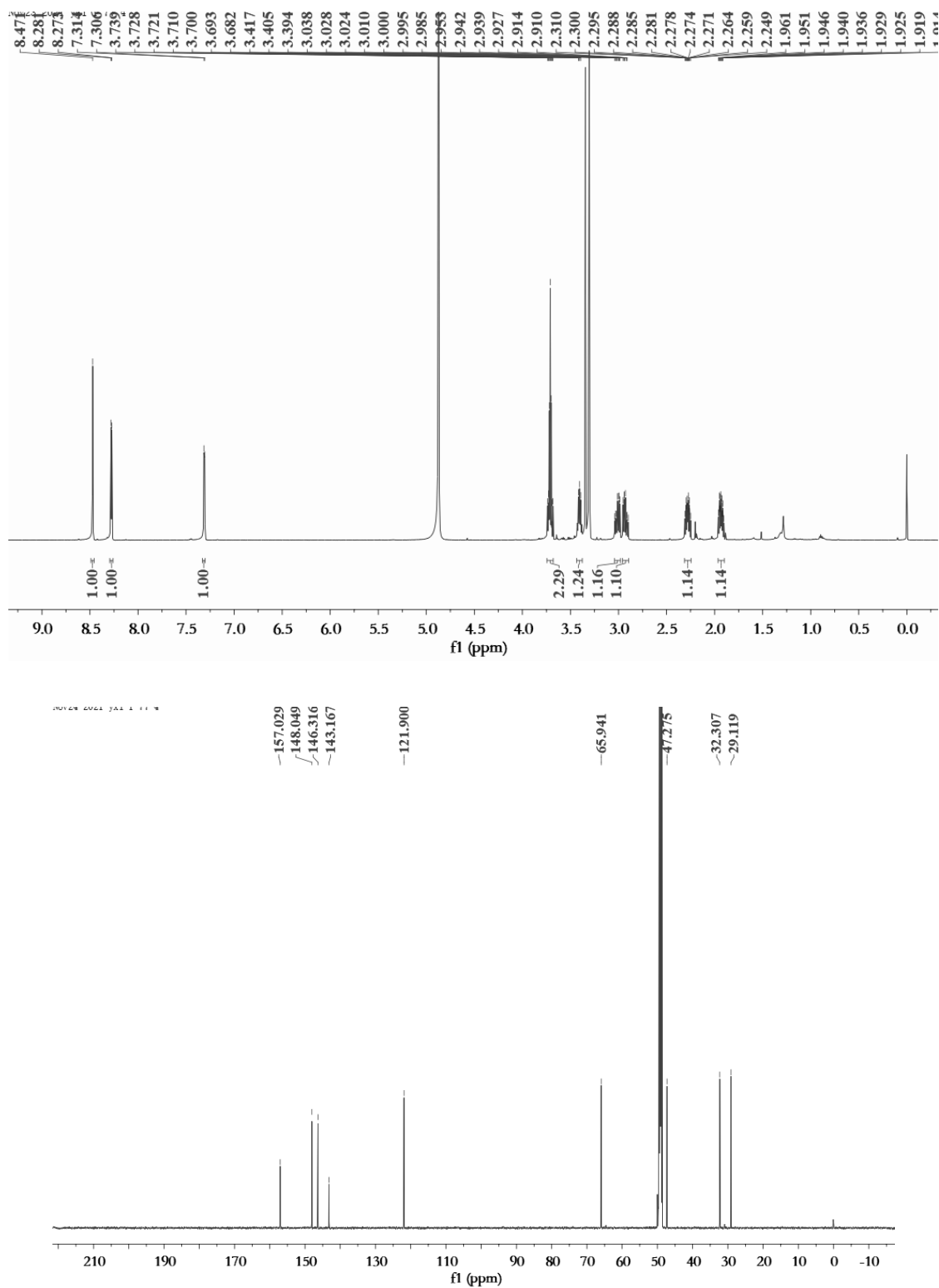


Figure S2: ¹H-NMR (600 MHz, CD₃OD) and ¹³C-NMR (150 MHz, CD₃OD) spectrum of **1**

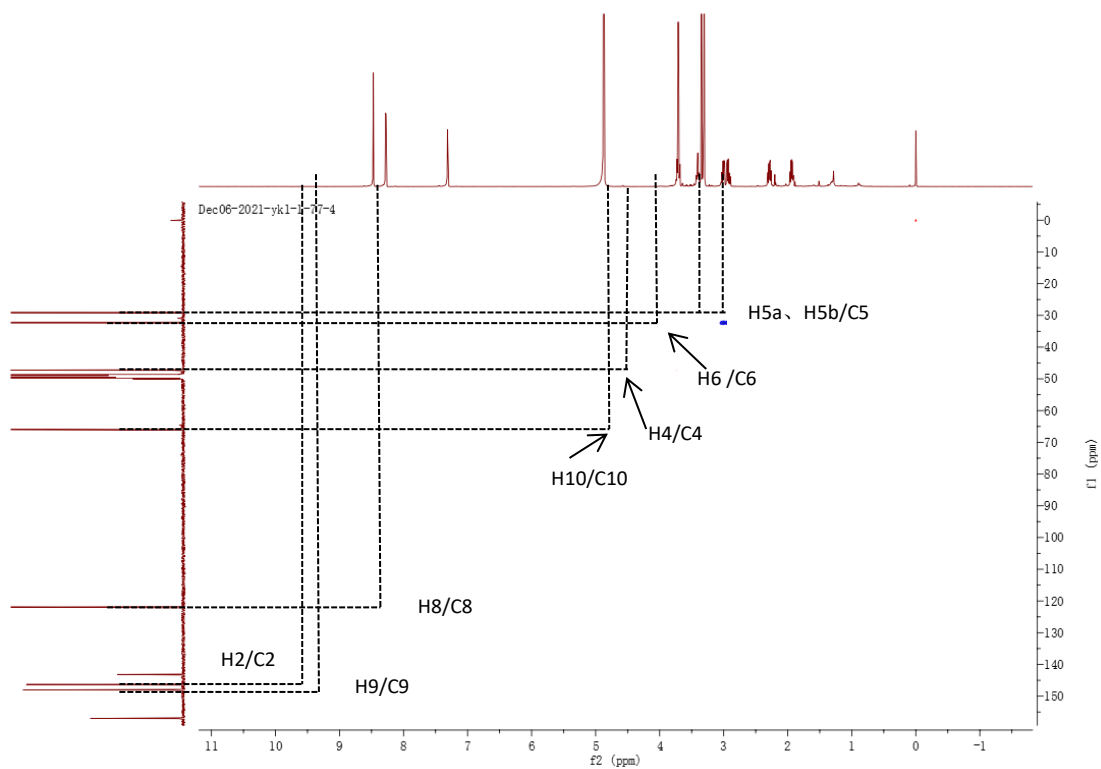


Figure S3: HSQC spectrum of 1

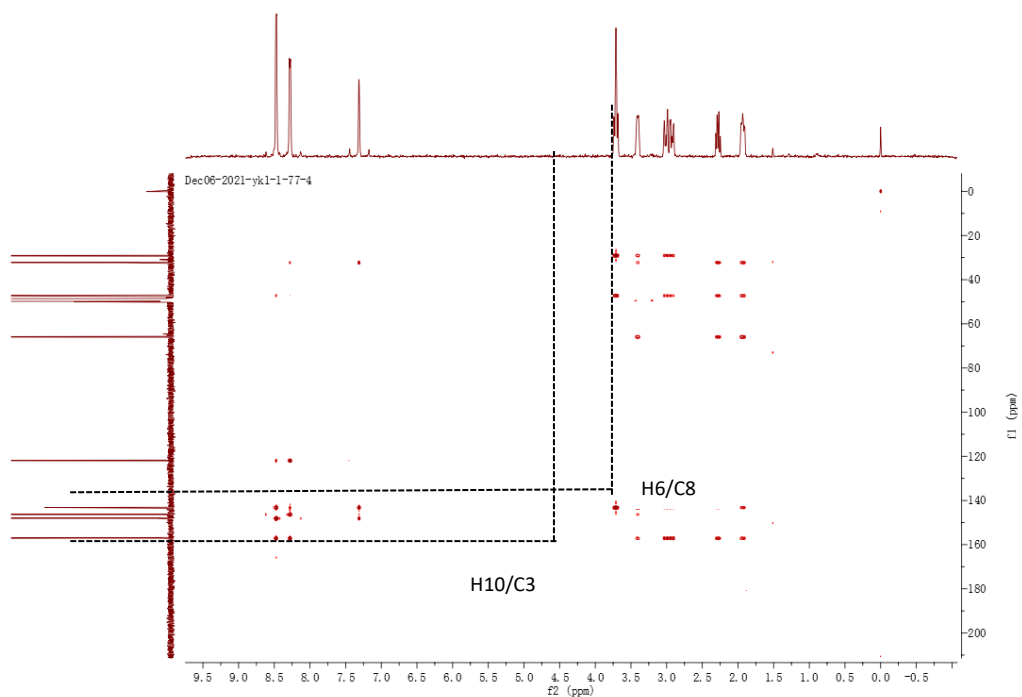


Figure S4: HMBC spectrum of 1

© 2022 ACG Publications. All rights reserved.

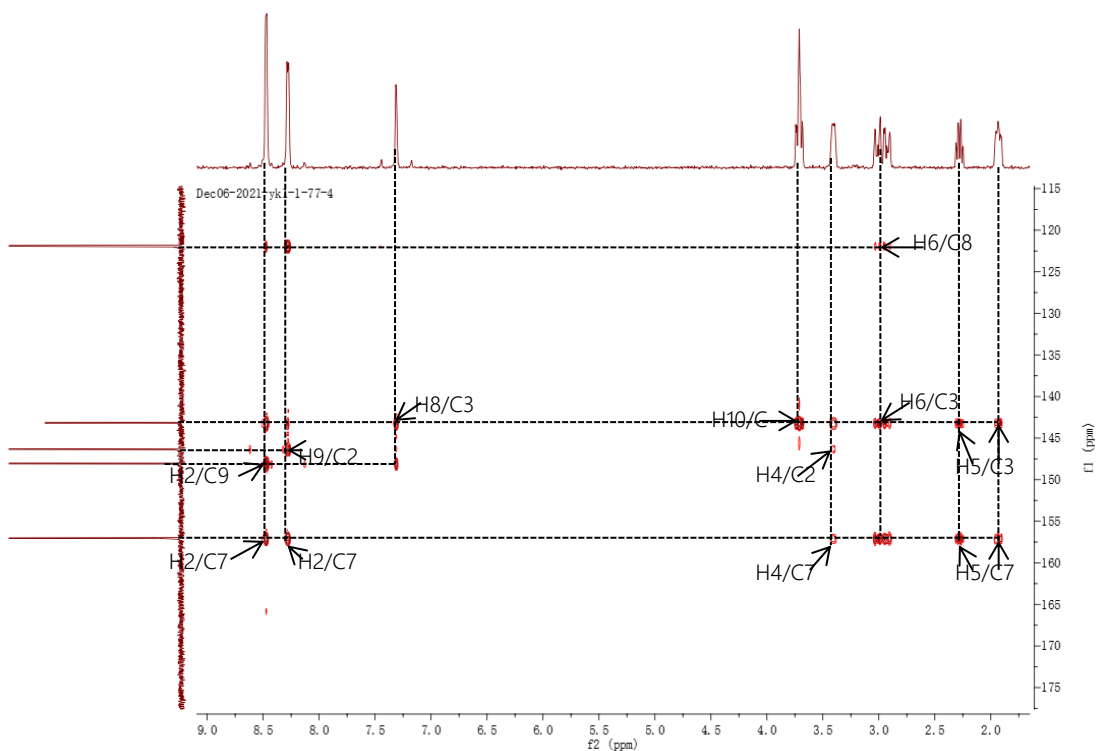


Figure S5: HMBC spectrum of **1** (From δ_C 115 ppm to δ_C 160 ppm)

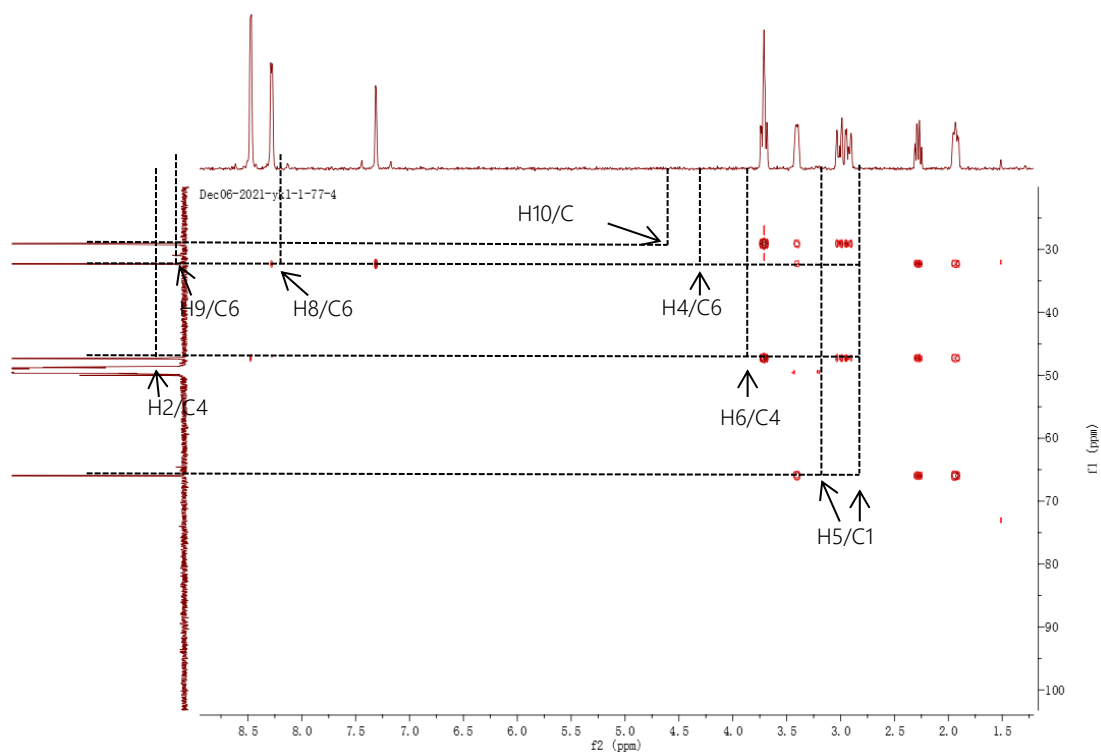


Figure S6: HMBC spectrum of **1** (From δ_C 25 ppm to δ_C 90 ppm)

© 2022 ACG Publications. All rights reserved.

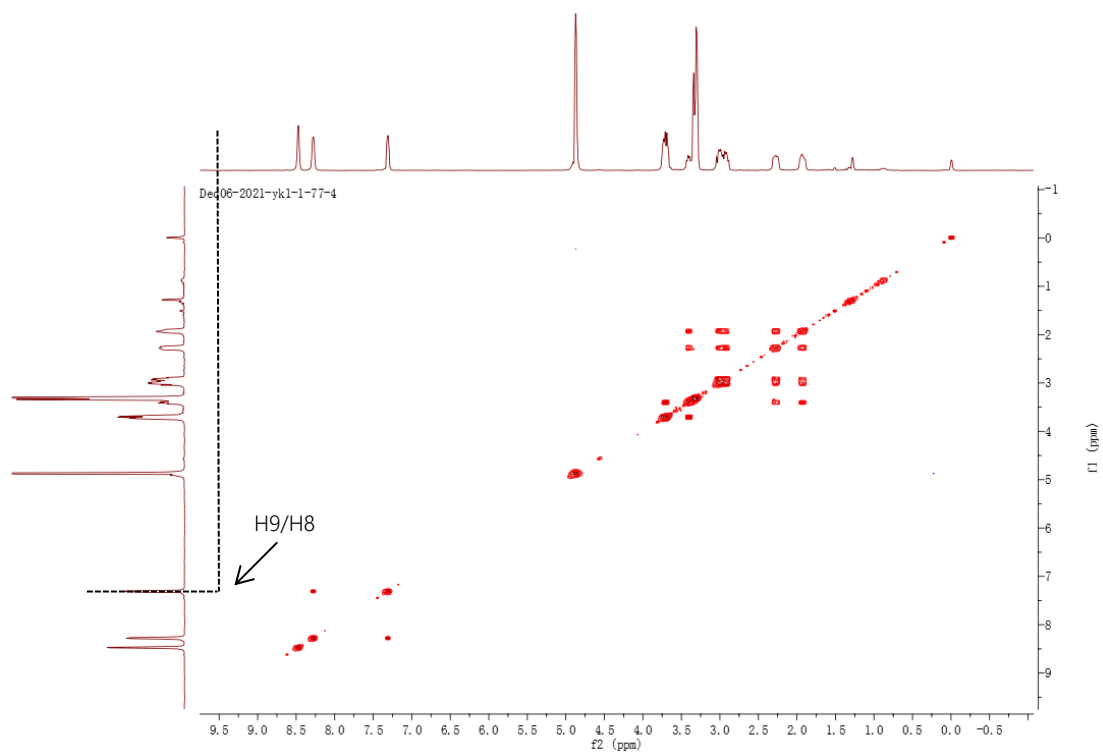


Figure S7: ^1H - ^1H COSY spectrum of **1**

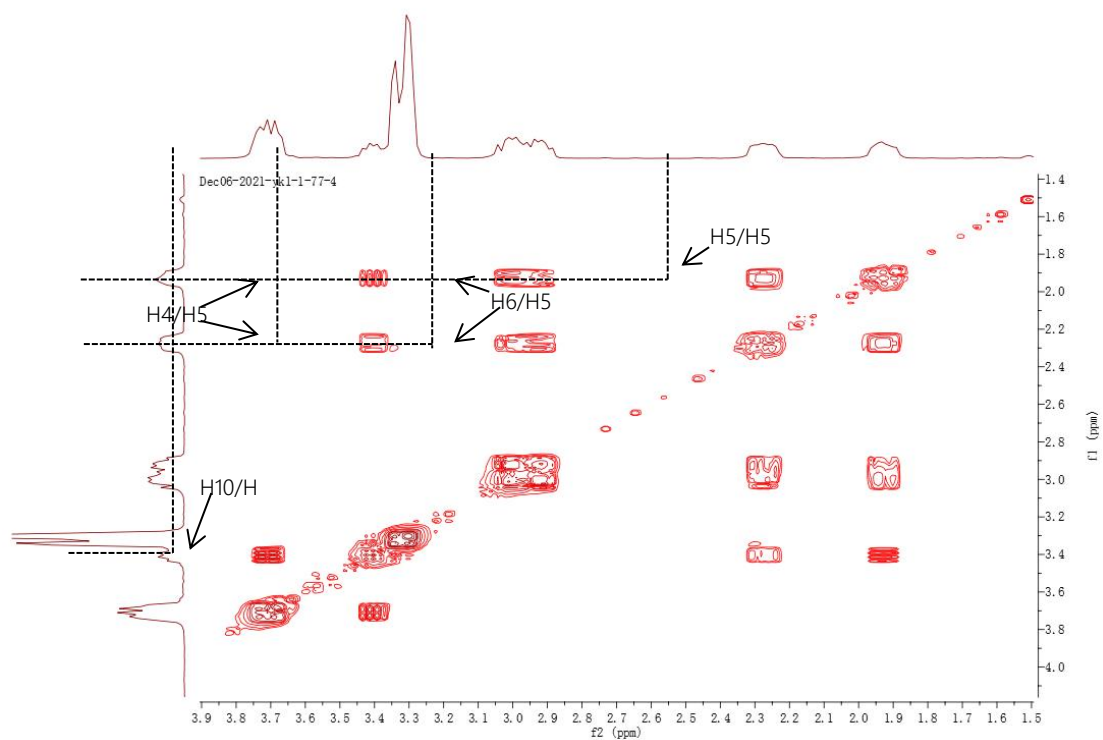


Figure S8: ^1H - ^1H COSY spectrum of **1**(From δ_{H} 1.5 ppm to δ_{H} 4.0 ppm)

© 2022 ACG Publications. All rights reserved.

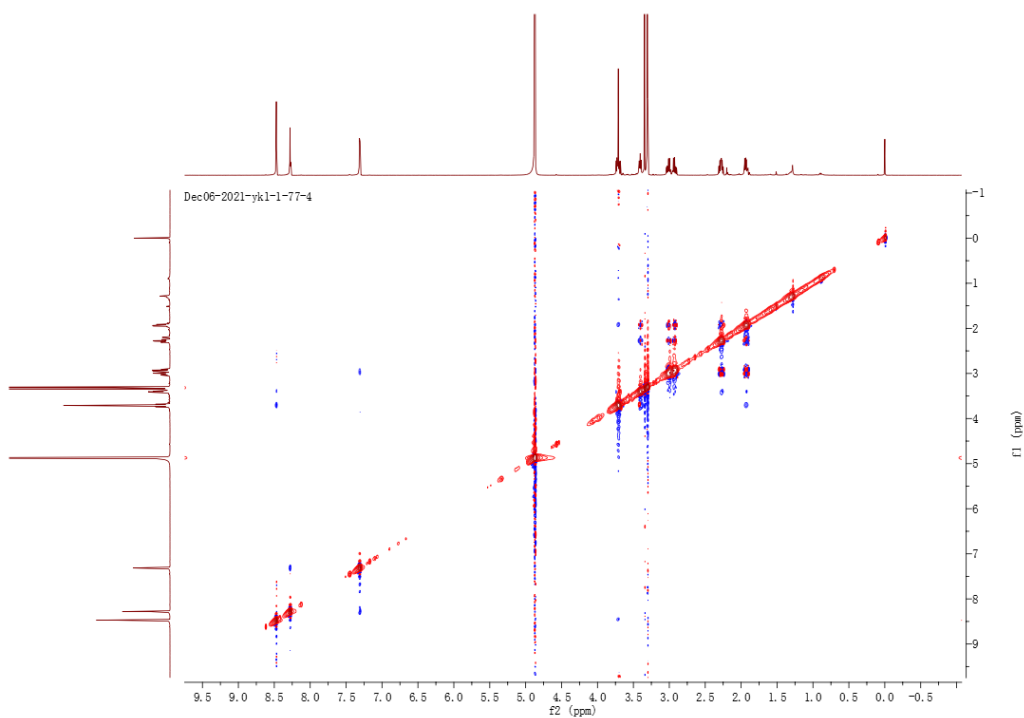


Figure S9: NOESY spectrum of **1**

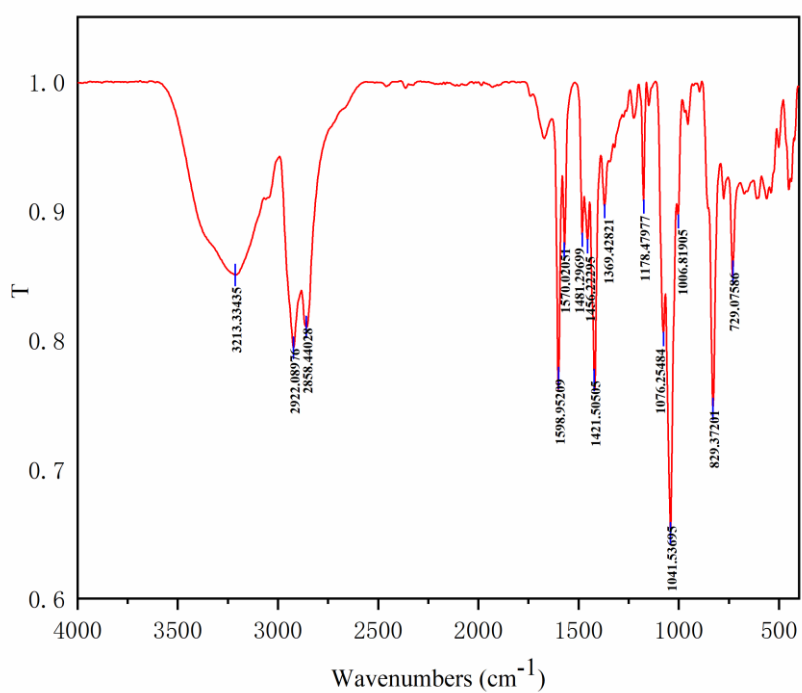


Figure S10: FT-IR spectrum of **1**

© 2022 ACG Publications. All rights reserved.

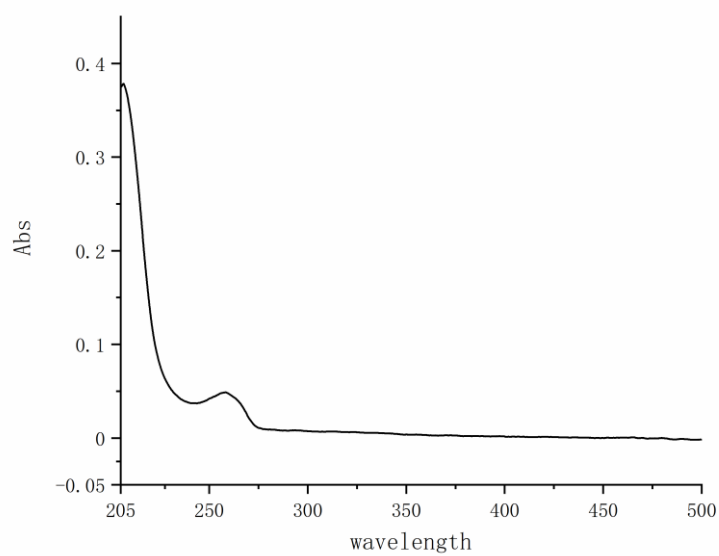


Figure S11: UV spectrum of **1**

SciFinder®

Page 2



Substances (0)

[View in SciFinder®](#)

We couldn't find any results. Please update your search query and try again.

Substances with (0) results

Copyright © 2022 American Chemical Society (ACS). All Rights Reserved.
Internal use only. Redistribution is subject to the terms of your SciFinder® License Agreement and CAS information Use Policies.

Figure S12: Scifinder search of new compound **1**

Apr15-2021-yk1-1-29-1

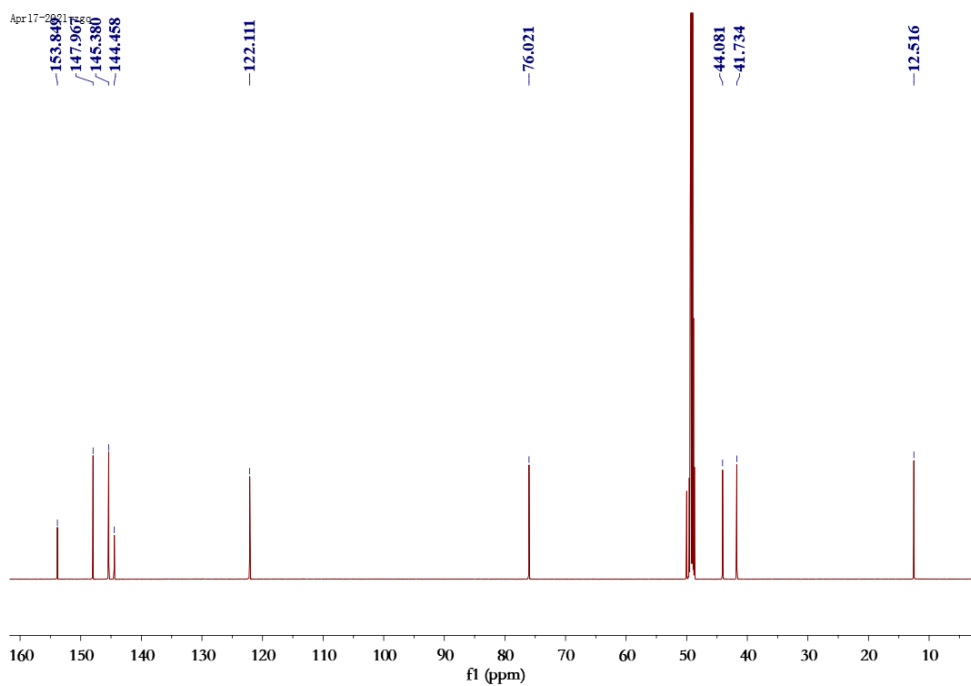
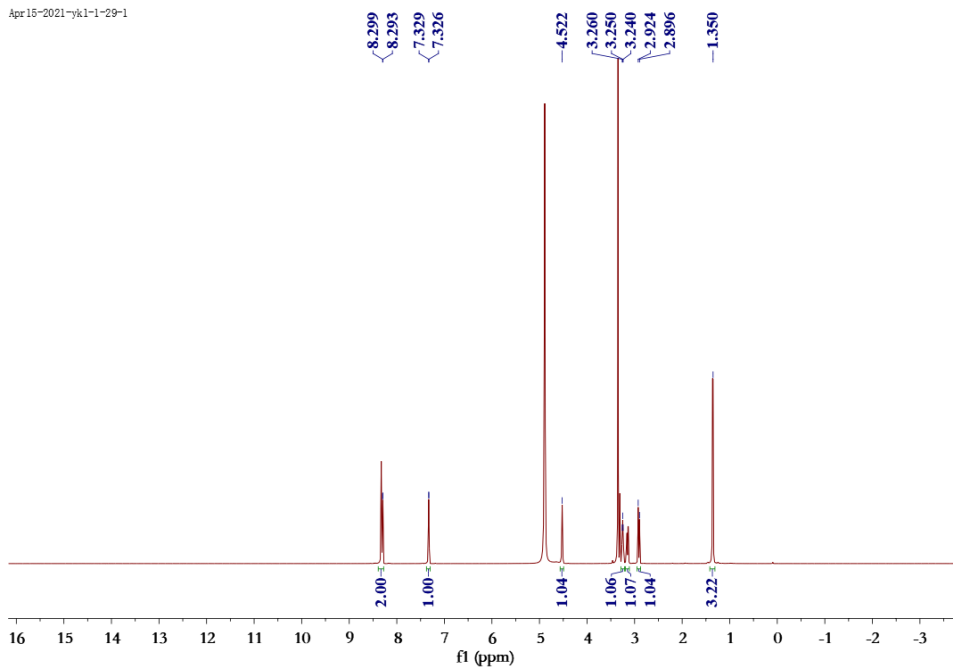


Figure S13: ¹H-NMR (600 MHz, CD₃OD) and ¹³C-NMR (150 MHz, CD₃OD) spectrum of **2**

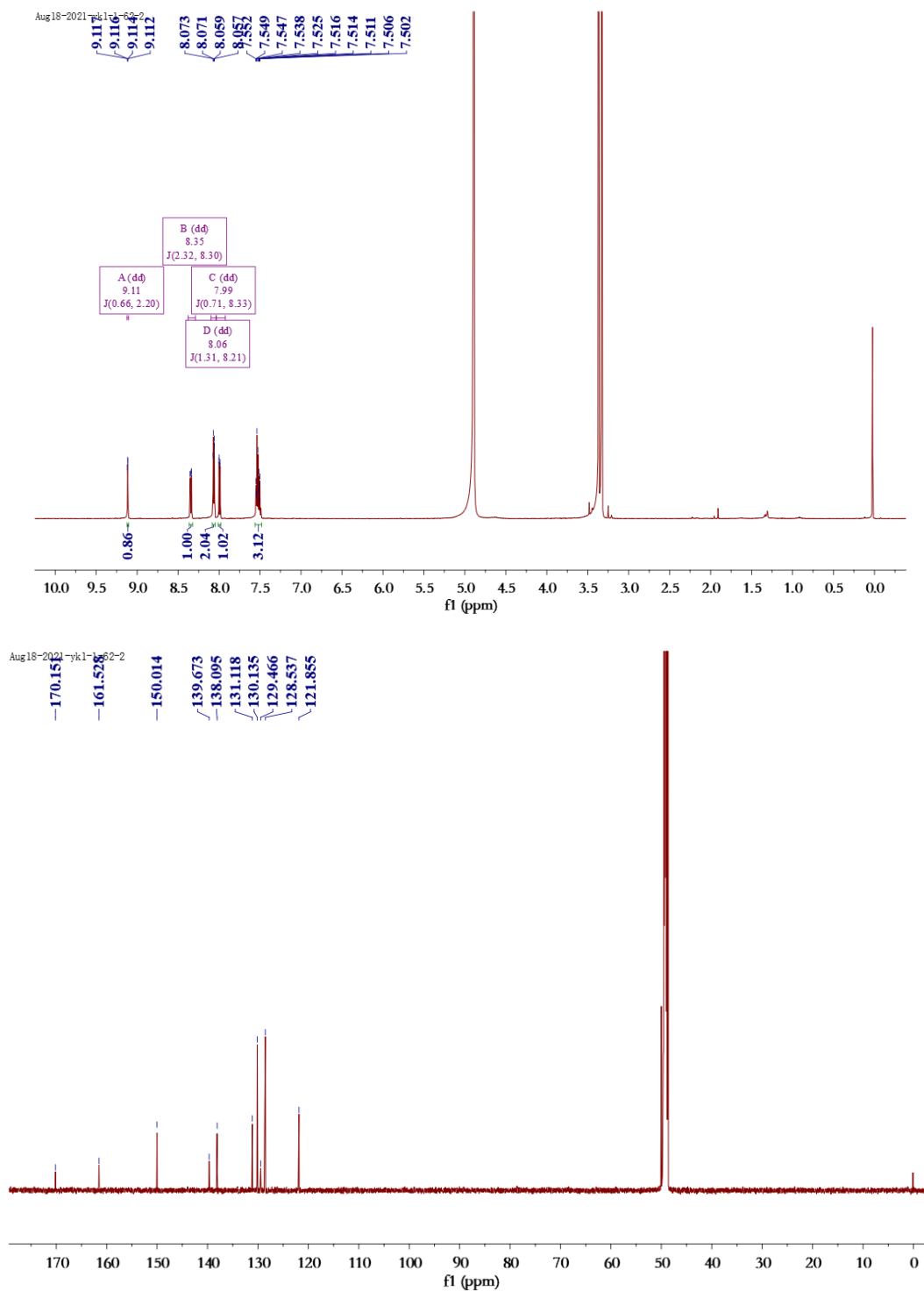


Figure S14: ¹H-NMR (600 MHz, CD₃OD) and ¹³C-NMR (150 MHz, CD₃OD) spectrum of **3**

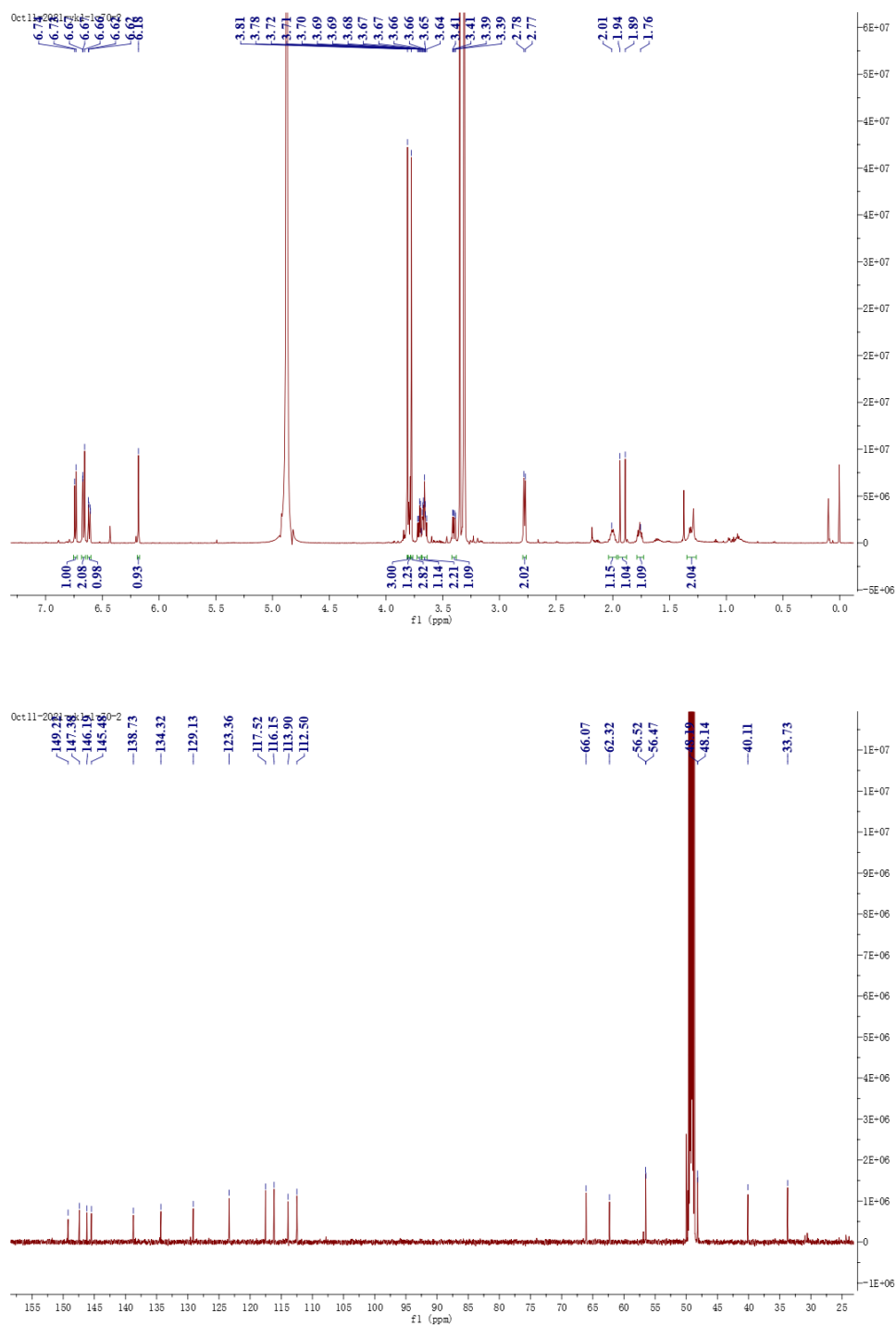


Figure S15: ¹H-NMR (600 MHz, CD₃OD) and ¹³C-NMR (150 MHz, CD₃OD) spectrum of **4**

© 2022 ACG Publications. All rights reserved.

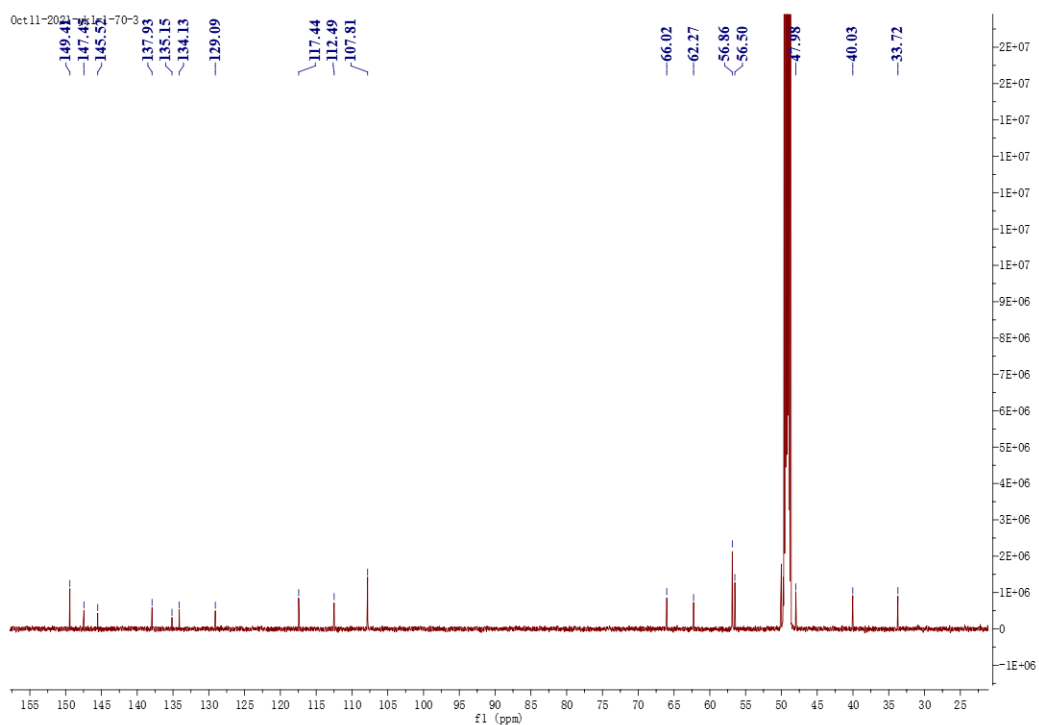
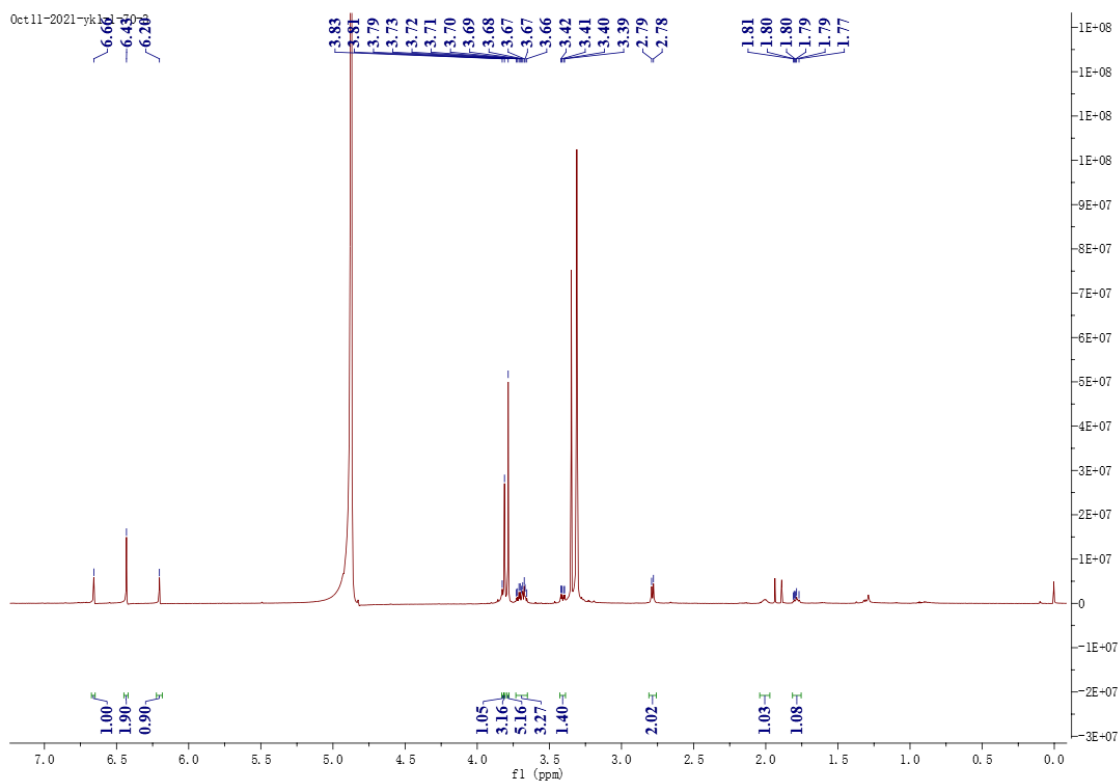


Figure S16: $^1\text{H-NMR}$ (600 MHz, CD_3OD) and $^{13}\text{C-NMR}$ (150 MHz, CD_3OD) spectrum of **5**

© 2022 ACG Publications. All rights reserved.

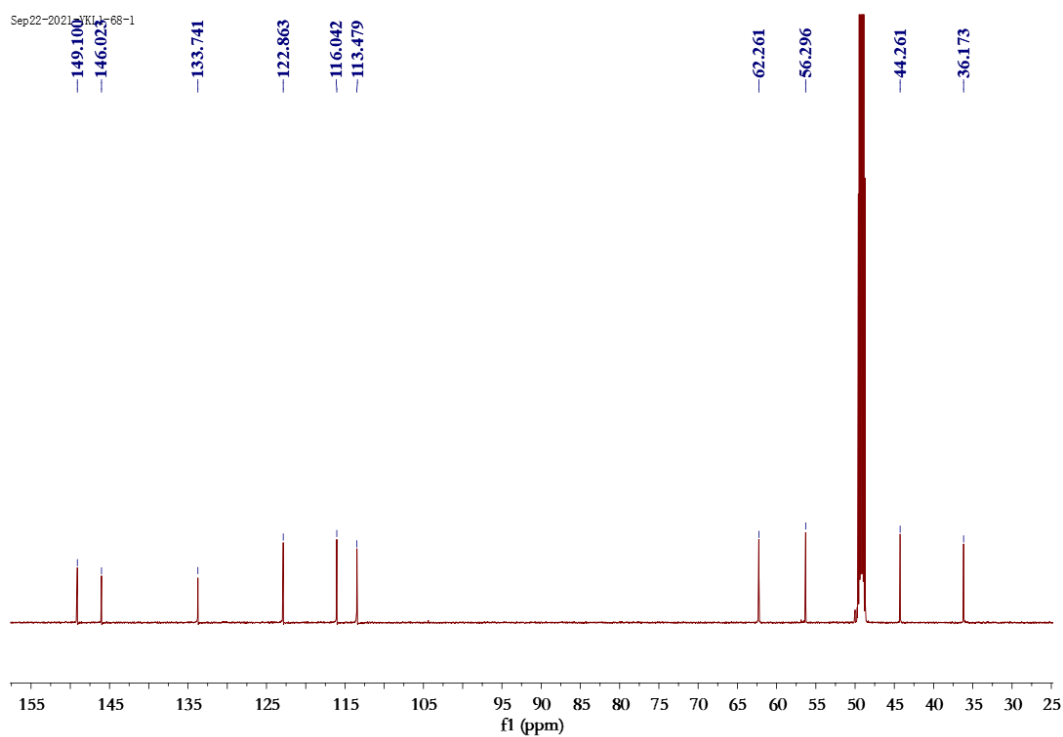
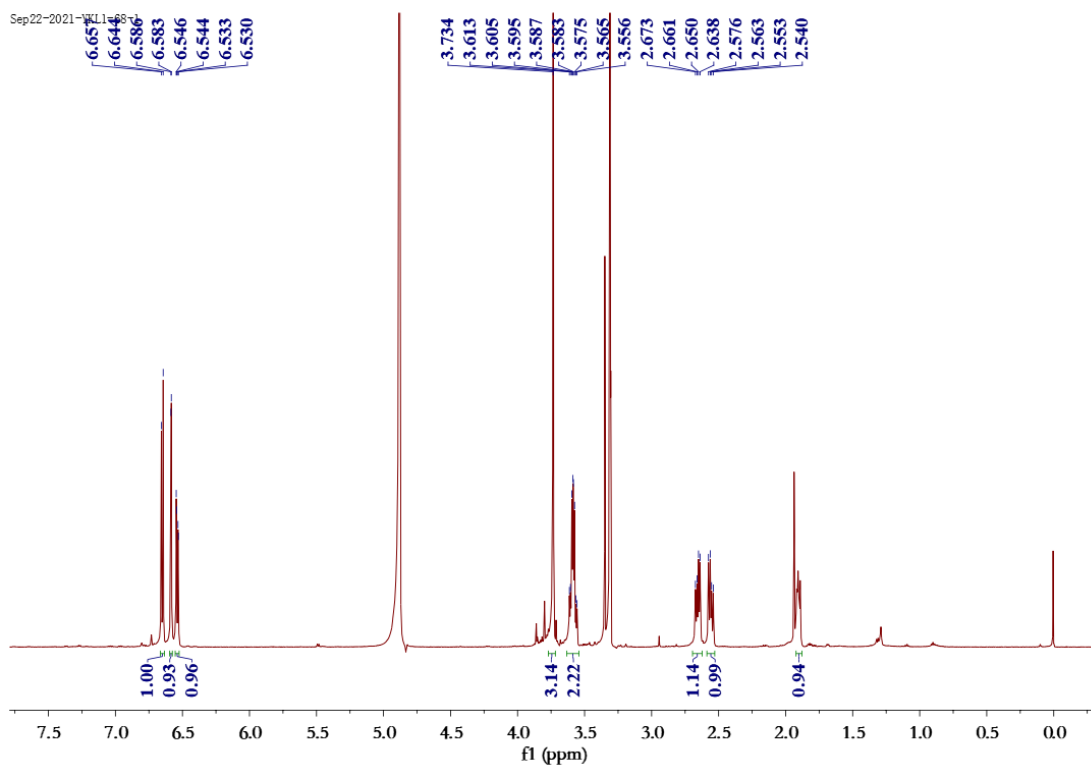


Figure S17: ^1H -NMR (600 MHz, CD_3OD) and ^{13}C -NMR (150 MHz, CD_3OD) spectrum of **6**

© 2022 ACG Publications. All rights reserved.

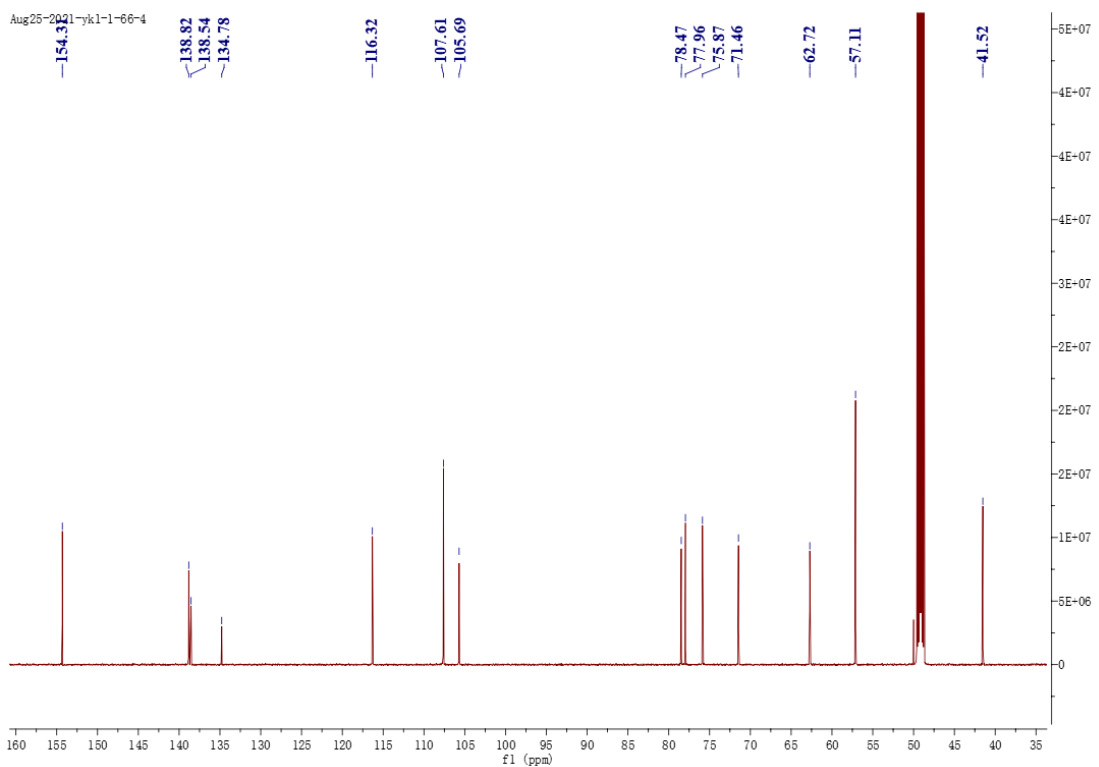
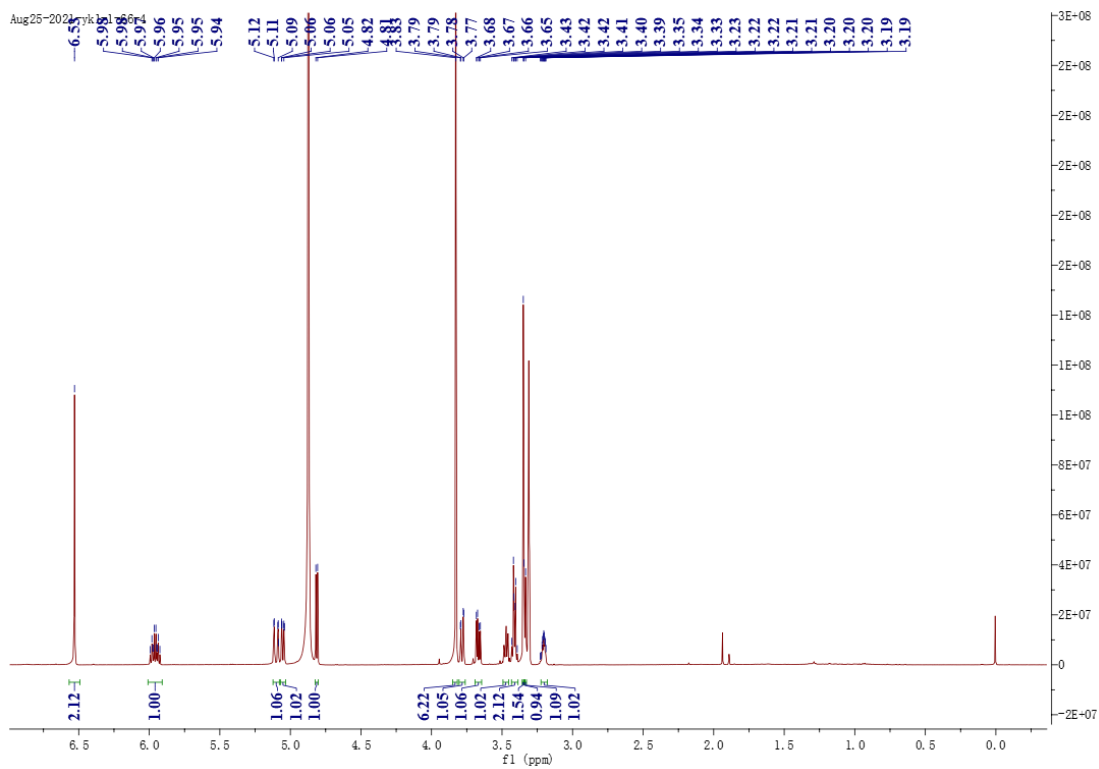


Figure S18: $^1\text{H-NMR}$ (600 MHz, CD_3OD) and $^{13}\text{C-NMR}$ (150 MHz, CD_3OD) spectrum of **7**

© 2022 ACG Publications. All rights reserved.

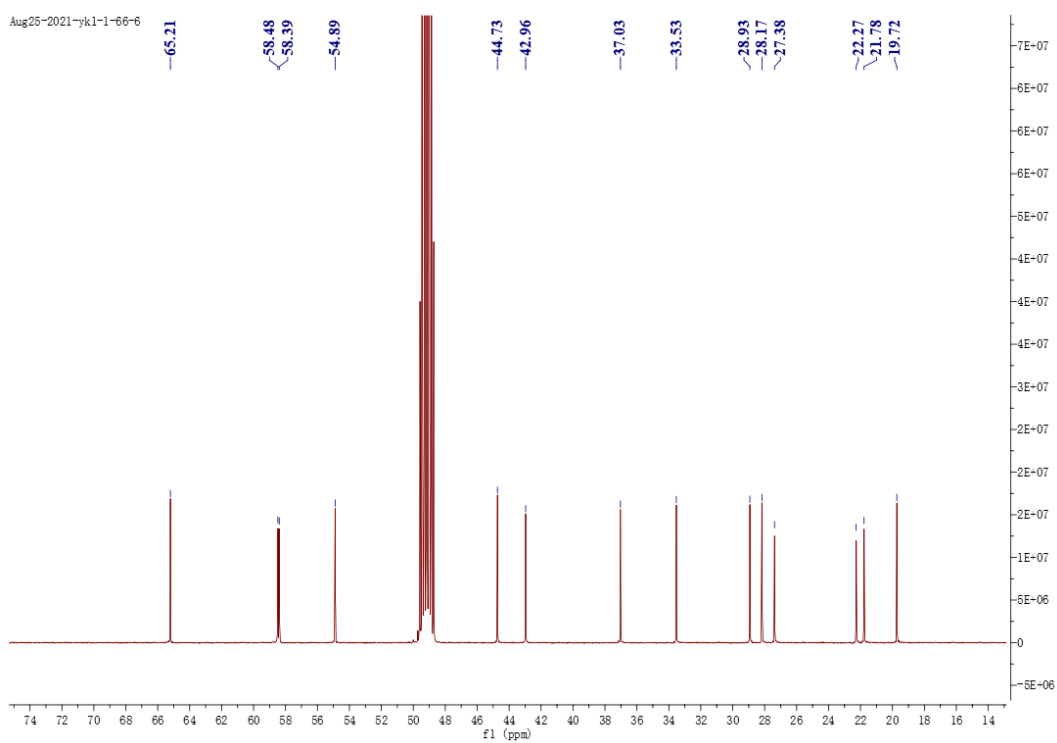
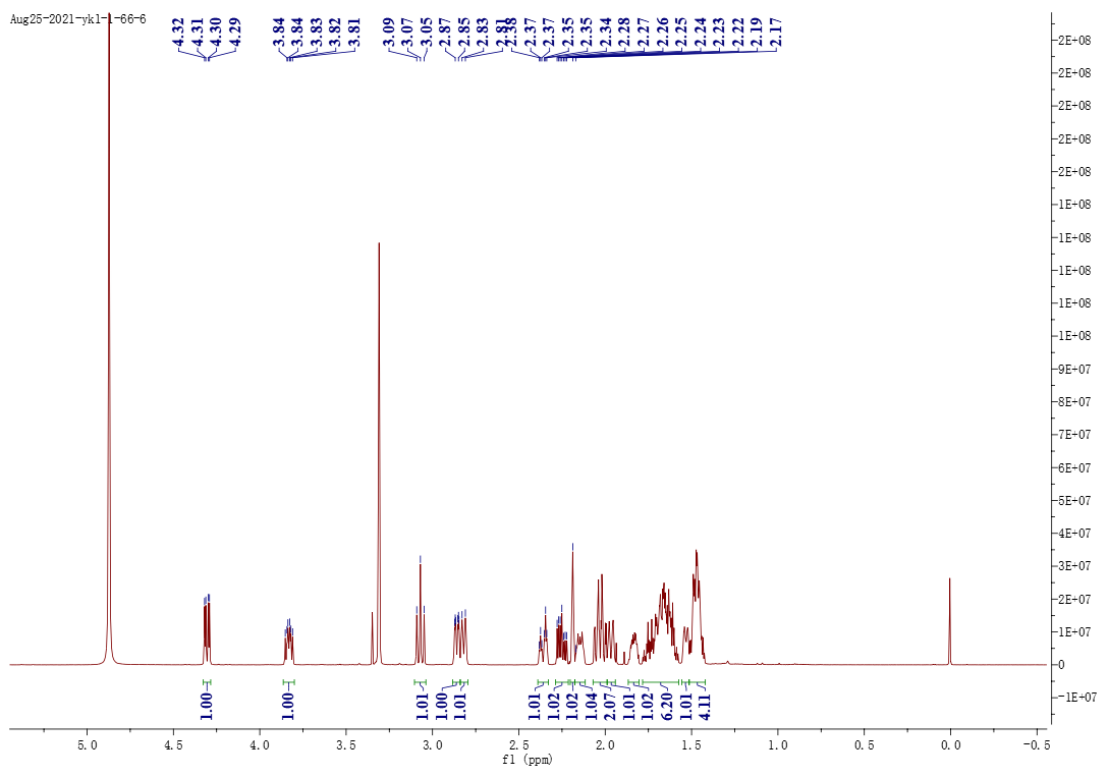


Figure S19: ^1H -NMR (600 MHz, CD_3OD) and ^{13}C -NMR (150 MHz, CD_3OD) spectrum of **8**

© 2022 ACG Publications. All rights reserved.

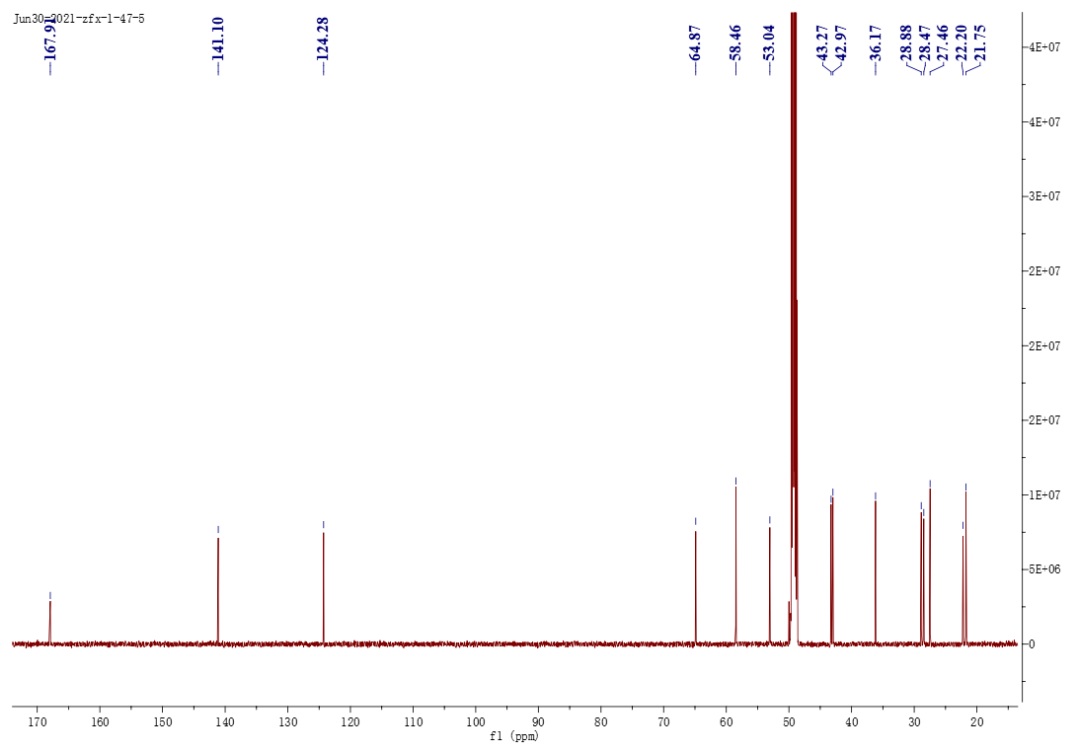
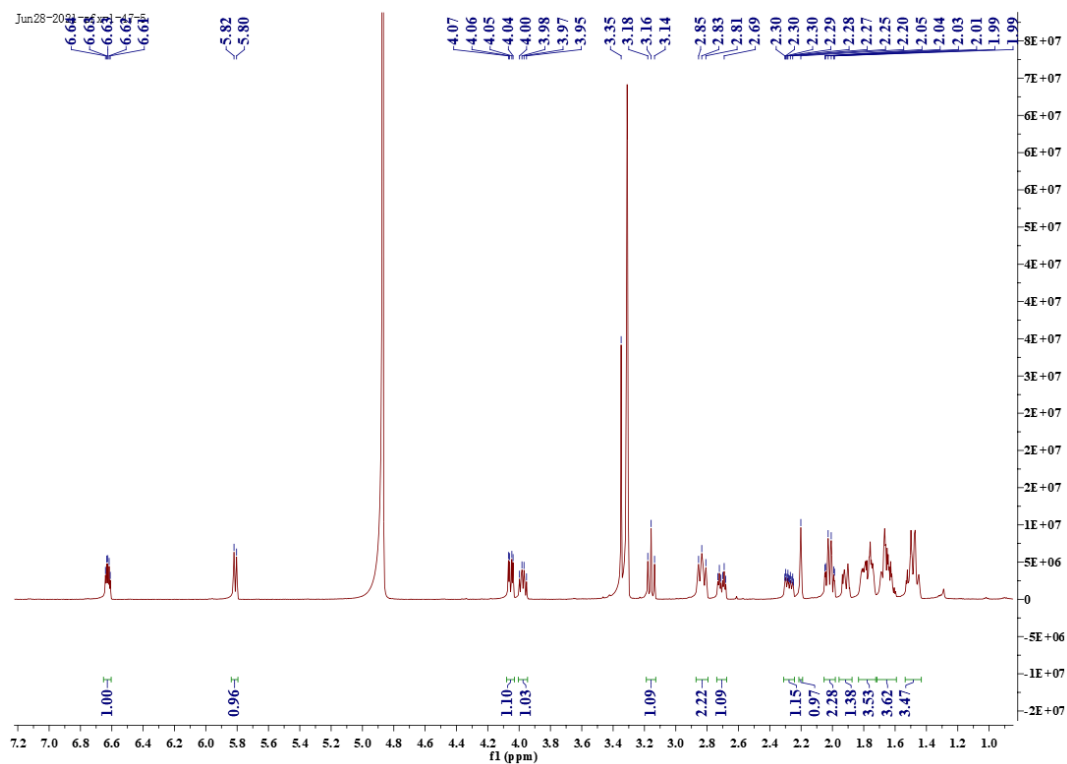


Figure S20: ^1H -NMR (600 MHz, CD_3OD) and ^{13}C -NMR (150 MHz, CD_3OD) spectrum of **9**

© 2022 ACG Publications. All rights reserved.

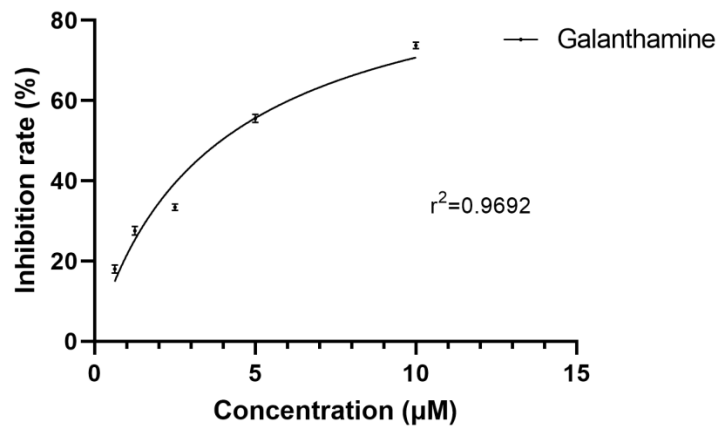


Figure S21: The inhibition rate curves of acetylcholinesterase inhibition activity

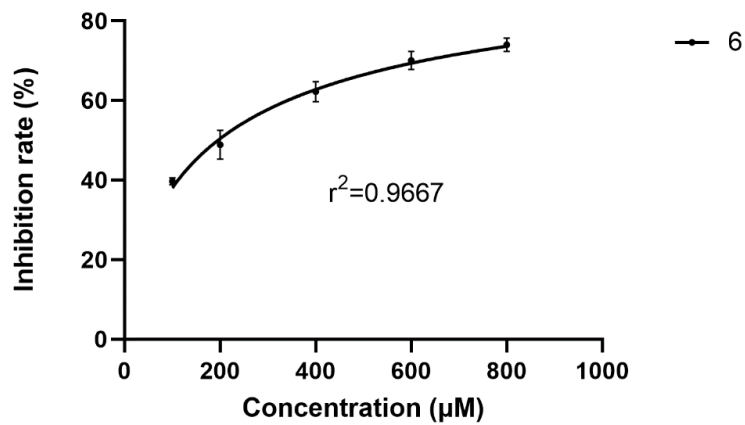
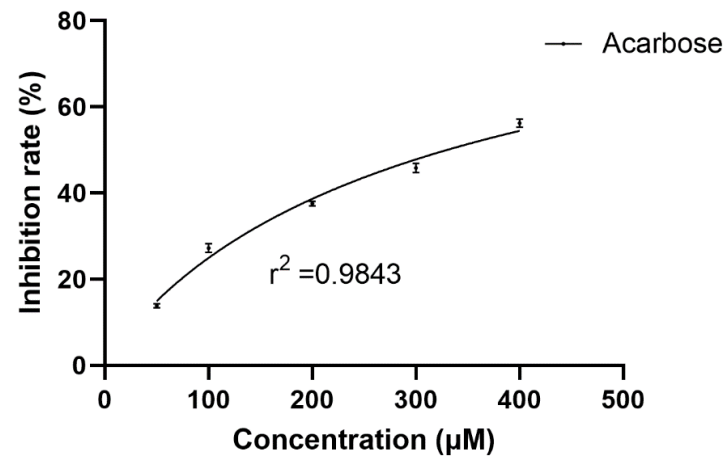


Figure S22: The inhibition rate curves of α -glucosidase inhibitory activity

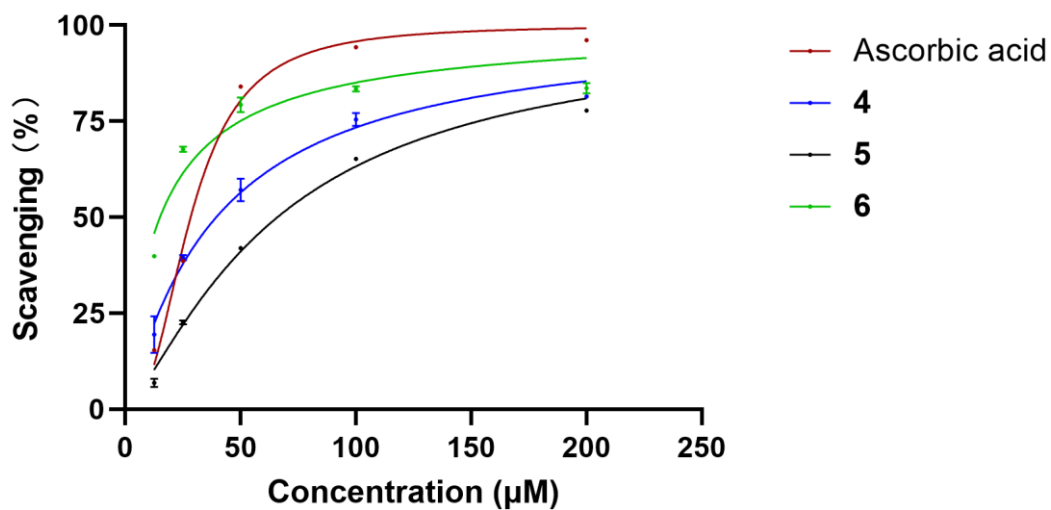


Figure S23: The inhibition rate curves of DPPH radical scavenging activity

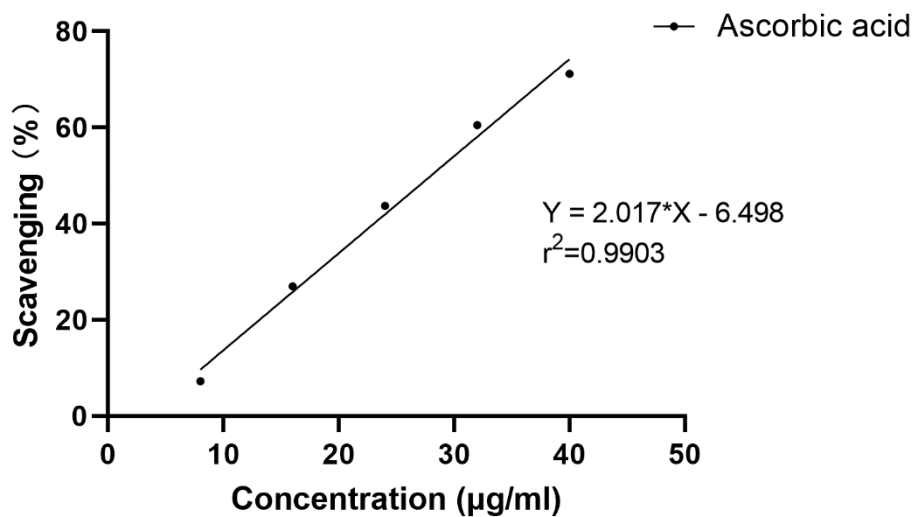
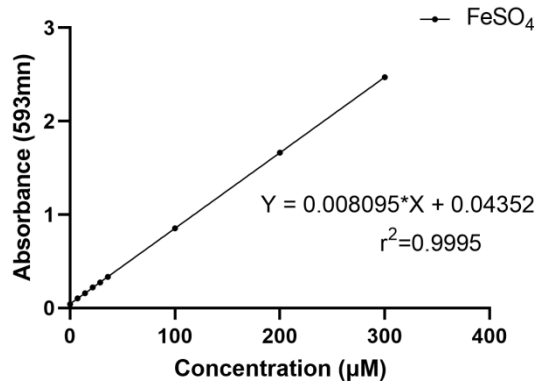
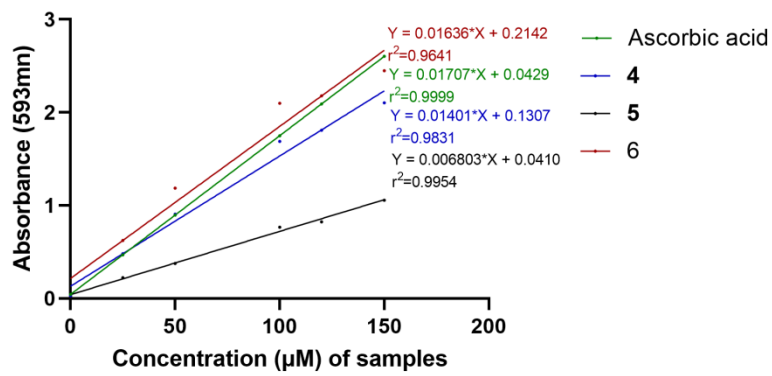


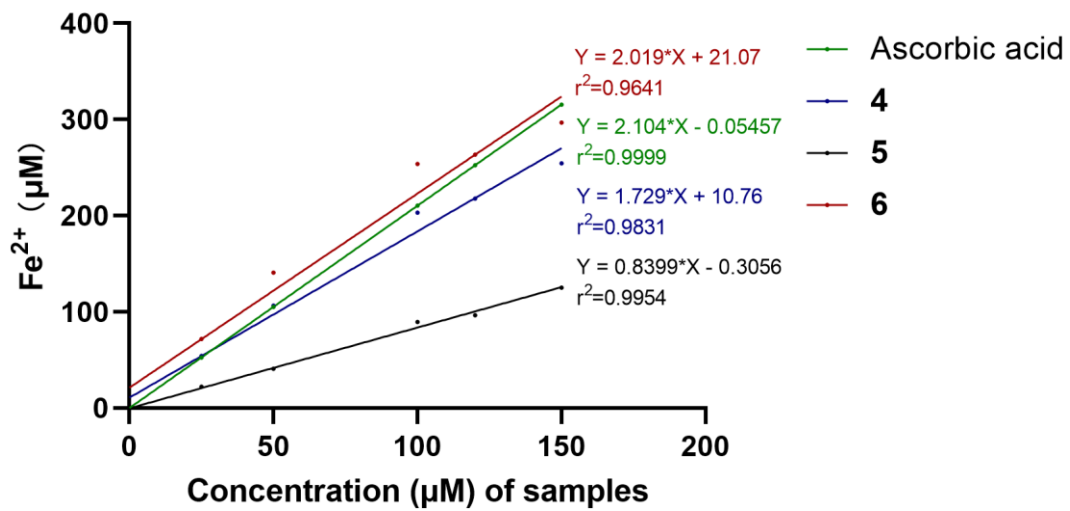
Figure S24: The inhibition rate curves of hydroxyl radical scavenging activity



(a)



(b)



(c)

Figure S25: The inhibition rate curves of FRAP activity

© 2022 ACG Publications. All rights reserved.

- (a) Liner regression analysis between FeSO₄ and absorbance at 593 nm ;
 (b) Liner regression analysis between samples and absorbance at 593 nm;
 (c) Liner regression analysis between samples and FeSO₄

Table S1: The inhibitory rates of compounds **1–9** at the test concentrations*

No.	AChE inhibition activity ^a	α -Glucosidase inhibitory activity ^b	DPPH radical scavenging capacity ^c	FRAP value ^d	Hydroxyl radical scavenging capacity ^e
	Inhibitory rates(%)	Inhibitory rates(%)	Scavenging rates(%)	$\mu\text{M Fe}^{2+}/250 \mu\text{M}$ samples	Scavenging rates(%)
1	0.09 ± 0.01	8.52 ± 1.04	0.32 ± 0.07	-6.06 ± 0.23	-4.39 ± 1.52
2	-2.62 ± 0.04	1.20 ± 1.71	5.00 ± 0.42	5.85 ± 0.31	-1.29 ± 0.38
3	-4.76 ± 0.05	5.71 ± 0.90	2.55 ± 0.32	-2.90 ± 0.18	1.46 ± 0.74
4	-8.21 ± 0.02	6.37 ± 0.47	85.70 ± 0.13	295.04 ± 1.48	-32.46 ± 2.16
5	-3.56 ± 0.04	-5.69 ± 0.18	83.27 ± 0.18	171.25 ± 1.40	-21.07 ± 2.27
6	-5.39 ± 0.06	41.08 ± 0.69	86.98 ± 0.14	317.73 ± 4.28	-33.37 ± 1.27
7	1.19 ± 0.01	-17.75 ± 0.23	-0.32 ± 0.52	-3.06 ± 0.48	0.12 ± 0.20
8	-3.79 ± 0.01	6.63 ± 1.15	1.22 ± 0.50	-5.32 ± 0.57	0.76 ± 0.37
9	-0.67 ± 0.02	-0.76 ± 0.51	1.92 ± 0.71	-0.44 ± 0.30	1.42 ± 0.46

*Result values are expressed as the mean ± SD (n = 3)

The test concentrations a: 100 μM ; b: 400 μM ; c: 200 μM ;

d: 250 μM (525.21 $\mu\text{M Fe}^{2+}/250 \mu\text{M}$ ascorbic acid); e:250 μM .

Table S2: Optical rotation value of **4–6** ($[\alpha]_D^{20}$)

Compounds	Optical rotation
4	16.8°
5	10.8°
6	-16.1°